





## COSMOLOGICAL EVOLUTION OF BIANCHI TYPE- $VI_0$ KANIADAKIS HOLOGRAPHIC DARK ENERGY MODEL

 B. Ganeswara Rao<sup>a,b</sup>,  Dipana Jyoti Mohanty<sup>b</sup>,  Y. Aditya<sup>c,\*</sup>,  U.Y. Divya Prasanthi<sup>d</sup>

<sup>a</sup>Department of Mathematics, Sri G.C.S.R. College, Rajam-532127, India

<sup>b</sup>Department of Mathematics, GIET University, Gunupur-765002, India

<sup>c</sup>Department of Mathematics, GMR Institute of Technology, Rajam-532127, India

<sup>d</sup>Department of Statistics & Mathematics, College of Horticulture, Dr. Y.S.R. Horticultural University, Parvathipuram-535502, India

\*Corresponding Author e-mail: [aditya.y@gmrit.edu.in](mailto:aditya.y@gmrit.edu.in); [yaditya2@gmail.com](mailto:yaditya2@gmail.com)

Received December 5, 2023; revised December 19, 2023; accepted January 10, 2024

The purpose of this paper is to construct an anisotropic and spatially homogeneous Bianchi type- $VI_0$  Kaniadakis holographic dark energy model in general relativity. For this purpose, we consider Hubble horizons as the IR cutoff. To obtain a deterministic solution of the model's field equations, we assume a relationship between the metric potentials which leads to an exponential solution and accelerated expansion. To investigate the physical behaviour of our dark energy model, we obtain some important cosmological parameters like Hubble, deceleration, equation of state and statefinder as well as  $\omega_{khde} - \omega'_{khde}$ ,  $r - s$  and  $r - q$  planes. We also included the stability analysis for the dark energy model through the squared speed of sound. It is observed that the equation of state parameter shows  $\Lambda$ CDM model at late times. Also, the squared speed of sound gives the stability of the Kaniadakis holographic dark energy model at the initial epoch and the model is unstable at late times. Statefinder diagnostic and deceleration parameters exhibit a smooth transition of the universe from the decelerating phase to the current accelerated expansion of the universe and also correspond to the  $\Lambda$ CDM model at late times. All these cosmological parameters support recent observational data.

**Keywords:** *Bianchi type- $VI_0$  model; Dark energy model; General theory of relativity; Cosmology; Kaniadakis holographic dark energy*

**PACS:** 98.80.-k, 95.36.+x

### 1. INTRODUCTION

Einstein's general relativity (GR) is regarded as a key theory for comprehending the concealed features of gravitational dynamics, which provide a fundamental comprehension of astrophysical events and the universe. Recent observations have provided compelling evidence that the universe undergoes both early inflation and late-time rapid expansion [1]-[3]. The phenomenon is attributed to the existence of an enigmatic force called dark energy (DE), which exhibits repulsive gravitational effects. There are primarily two methods to addressing the enigmatic characteristics of dark energy and cosmic acceleration problems. Modified theories of gravity are different attempts to integrate dark energy by modifying the action principle in general relativity. In an alternative approach, many dynamical dark energy candidates are offered in order to comprehend the essence of dark energy. Both updated theories of gravity and dynamical DE models have received quite positive evaluations [4]-[7]. Of the several dynamical dark energy theories, the primary contender is the cosmological constant. However, it is plagued by issues of cosmic coincidence and fine-tuning. Due to this rationale, many alternative dynamical differential equation (DE) models have been proposed, including a range of scalar field models such as K-essence, phantom, quintessence, ghost, etc., as well as Chaplygin gas and holographic DE models [8]-[14].

Among the several dynamical DE models, the holographic dark energy model has gained popularity as a preferred method to investigate the riddle of dark energy. The proposal is based on the quantum characteristics of black holes, which have been thoroughly studied in the literature to research quantum gravity [13, 14]. As per the holographic principle, the vacuum energy  $\Lambda$  of a system of size  $L$  must not exceed the mass of a black hole of the same size, since this would result in the development of a black hole in quantum field theory. The energy density of HDE is determined according to the formulation provided by Cohen et al. [15]

$$\rho_{khde} = 3d^2 m_p^2 L^{-2}. \quad (1)$$

where  $m_p$  represents the reduced Planck mass,  $3d^2$  denotes a numerical constant, and  $L$  represents the IR-cutoff. Various forms of IR-cutoff have been examined in the scholarly literature, such as the Hubble horizon  $H^{-1}$ , event

**Cite as:** B.G. Rao, D.J. Mohanty, Y. Aditya, U.Y.D. Prasanthi, East Eur. J. Phys. 1, 43 (2024), <https://doi.org/10.26565/2312-4334-2024-1-03>

© B.G. Rao, D.J. Mohanty, Y. Aditya, U.Y.D. Prasanthi, 2024; CC BY 4.0 license

horizon, particle horizon, conformal universe age, Ricci scalar radius, and Granda–Oliveros cutoff [16]- [18]. The HDE models, with different IR cutoffs, provide a contemporary understanding of the universe’s acceleration. They also demonstrate that the transition redshift value, which marks the move from an earlier deceleration phase ( $q>0$ ) to the present acceleration phase ( $q<0$ ), aligns with modern observational evidence. Nojiri and Odintsov [19] introduced a method for combining the early and late stages of the universe using generalized HDE and phantom cosmology. They have recently extended this concept to what they call Hinflation [20] In recent times, many formulations of entropy have been used to create and examine cosmological models. Several novel models of holographic dark energy (HDE) have been developed, including the Tsallis HDE [21, 22], Sharma-Mittal HDE [23], and Renyi HDE model [24]. Several writers have examined several cosmological models of new HDE models [25]- [33]. Recently, the Kaniadakis statistics, which serves as a generalized measure of entropy [34]- [36], has been used to investigate various gravitational and cosmological implications. The generalized  $\mathcal{K}$ -entropy (Kaniadakis), which represents the entropy of a black hole, may be determined using a single free parameter [37]

$$S_{\mathcal{K}} = \frac{1}{\mathcal{K}} \sinh(\mathcal{K}S_{BH}) \tag{2}$$

where  $\mathcal{K}$  is an unknown parameter. Thus, by using the concept of entropy and the notion of holographic dark energy, a novel model of dark energy called Kaniadakis holographic dark energy (KHDE) is proposed [37], which exhibits significant characteristics. Jawad and Sultan [38], Sharma [39], and Drepanou et al. [40] have examined KHDE models inside various gravitational theories. The dynamic structures of HDE, as investigated by Sadeghi et al. [41], have been analyzed within the context of Brans-Dicke’s theory of gravity, using the Tsallis and Kaniadakis approaches.

Theoretical cosmology has shown increasing interest in anisotropic and spatially homogeneous worlds in recent decades. The primary empirical data from CMBR (Bennett et al. [42]) has been deemed as evidence in favor of a shift from a non-uniform phase of the universe to a uniform phase (Akarsu and Kilinc [43]). Furthermore, there is a belief that during the first stages of the universe, the isotropic FRW model may not provide a comprehensive and accurate depiction of matter. To conduct a realistic analysis of cosmological models and determine whether they can reach the observed level of homogeneity and isotropy, it is necessary to consider space-times that are both spatially homogeneous and anisotropic. Bianchi type (BT) cosmological models, which are homogeneous but not necessarily isotropic, have garnered significant attention from academics because to their anisotropic nature. Recently, several academics have developed intriguing cosmological models that include dark energy in the context of anisotropic Bianchi space-times. Various scholars have examined anisotropic cosmological models in diverse contexts [44]- [60].

Motivated by the above investigations and discussion, in this work, we consider BT- $VI_0$  space-time filled with matter and KHDE in the framework of GR. The work in this paper is configured as follows: In Sec. 2, the BT- $VI_0$  metric is given and the field equations in the presence of anisotropic KHDE fluid and matter are derived. Also, we obtained the solution of the field equations and constructed the KHDE model. Sec. 3 contains several cosmological parameters of our model. The results are summarised with conclusions in the last section.

## 2. FIELD EQUATIONS AND KANIADAKIS HDE MODEL

Einstein’s general theory of relativity is usually regarded as one of the most accomplished theories of gravity in contemporary physics. The salient feature of GR is its enduring constancy, which has been unaltered for over a century. The equations governing the field in this theory are expressed as

$$R_{ij} - \frac{1}{2}Rg_{ij} = -\frac{8\pi G}{c^4}T_{ij} \tag{3}$$

where  $R_{ij}$  is the Ricci tensor,  $T_{ij}$  is the energy–momentum tensor of matter distribution,  $G$  is Newton’s gravitational constant,  $R$  is Ricci scalar,  $g_{ij}$  is metric potential, and  $c$  is the speed of light. Here we assume the gravitational constants  $8\pi G=c=1$ . We consider the geometry of the universe as spatially homogeneous and anisotropic BT- $VI_0$  line element which can be written as

$$ds^2 = dt^2 - A^2 dx^2 - B^2 e^{2x} dy^2 - C^2 e^{-2x} dz^2, \tag{4}$$

where  $A$ ,  $B$  and  $C$  are functions of cosmic time  $t$  only. The following are the some of physical parameters which are useful in finding the solution of field equations for the BT- $VI_0$  space-time given by Eq. (4).

The average scale factor  $a(t)$  and volume  $V$  of the BT- $VI_0$  space-time are defined as

$$V = [a(t)]^3 = ABC. \tag{5}$$

Anisotropic parameter  $A_h$  is given by

$$A_h = \frac{1}{3} \sum_{i=1}^3 \left( \frac{H_i - H}{H} \right)^2 \tag{6}$$

where  $H_1 = \frac{\dot{A}}{A}$ ,  $H_2 = \frac{\dot{B}}{B}$ ,  $H_3 = \frac{\dot{C}}{C}$  are directional Hubble's parameters and  $H = \frac{1}{3} \left( \frac{\dot{A}}{A} + \frac{\dot{B}}{B} + \frac{\dot{C}}{C} \right)$  is mean Hubble's parameter. Here and after an overhead dot denotes differentiation concerning cosmic time  $t$ . Expansion scalar ( $\theta$ ) and shear scalar ( $\sigma^2$ ) are defined as

$$\theta = u_{;i}^i = \frac{\dot{A}}{A} + \frac{\dot{B}}{B} + \frac{\dot{C}}{C} \quad (7)$$

$$\sigma^2 = \frac{1}{2} \sigma^{ij} \sigma_{ij} = \frac{1}{3} \left( \frac{\dot{A}^2}{A^2} + \frac{\dot{B}^2}{B^2} + \frac{\dot{C}^2}{C^2} - \frac{\dot{A}\dot{B}}{AB} - \frac{\dot{A}\dot{C}}{AC} - \frac{\dot{B}\dot{C}}{BC} \right) \quad (8)$$

where

$$\sigma_{ij} = \frac{1}{2} (u_{i;\mu} h_j^\mu + u_{j;\mu} h_i^\mu) - \frac{1}{3} \theta h_{ij}, \quad (9)$$

with  $h_{ij} = g_{ij} - u_i u_j$  is the projection tensor while  $u_i = (1, 0, 0, 0)$  is the four-velocity in the comoving coordinates. The deceleration parameter is given by

$$q = \frac{d}{dt} \left( \frac{1}{H} \right) - 1. \quad (10)$$

The matter distribution is assumed to be the combination of pressure-less matter and anisotropic DE which are, respectively, given as

$$T'_{ij} = \rho_m u_i u_j \quad (11)$$

$$\bar{T}_{ij} = (\rho_{khde} + p_{khde}) u_i u_j - p_{khde} g_{ij}. \quad (12)$$

where  $p_{khde}$  and  $\rho_{khde}$  are the pressure and energy density of DE fluid whereas  $\rho_m$  is the energy density of matter. The EoS parameter  $\omega_{khde}$  of DE is defined as  $\omega_{khde} = \frac{p_{khde}}{\rho_{khde}}$ . To ensure the present acceleration of the universe, here, we consider the anisotropic distribution of DE. After parameterizing the energy-momentum tensor of DE  $\bar{T}_{ij}$ , it can be expressed as follows:

$$\begin{aligned} \bar{T}_{ij} &= [1, -\omega_x, -\omega_y, -\omega_z] \rho_{khde} \\ &= [1, -\omega_{khde}, -(\omega_{khde} + \alpha), -(\omega_{khde} + \beta)] \rho_{khde} \end{aligned} \quad (13)$$

where  $\omega_x = \omega_{khde}$ ,  $\omega_y = \omega_{khde} + \alpha$  and  $\omega_z = \omega_{khde} + \beta$  are the directional equation of state (EoS) parameters on  $x$ ,  $y$  and  $z$  respectively. Here,  $\alpha$  and  $\gamma$  are the deviations from EoS parameter  $\omega_{khde}$  in  $y$  and  $z$  directions respectively.

In the comoving coordinate system, with the help of (13), the field equations (3) for the metric (4) can be written as

$$\frac{\ddot{B}}{B} + \frac{\ddot{C}}{C} + \frac{\dot{B}\dot{C}}{BC} + \frac{1}{A^2} = -\omega_{khde} \rho_{khde} \quad (14)$$

$$\frac{\ddot{A}}{A} + \frac{\ddot{C}}{C} + \frac{\dot{A}\dot{C}}{AC} - \frac{1}{A^2} = -(\omega_{khde} + \alpha) \rho_{khde} \quad (15)$$

$$\frac{\ddot{A}}{A} + \frac{\ddot{B}}{B} + \frac{\dot{A}\dot{B}}{AB} - \frac{1}{A^2} = -(\omega_{khde} + \beta) \rho_{khde} \quad (16)$$

$$\frac{\dot{A}\dot{B}}{AB} + \frac{\dot{B}\dot{C}}{BC} + \frac{\dot{A}\dot{C}}{AC} - \frac{1}{A^2} = \rho_{khde} + \rho_m \quad (17)$$

$$\frac{\dot{B}}{B} - \frac{\dot{C}}{C} = 0 \quad (18)$$

and, also, the energy conservation equation  $(T'_{ij} + \bar{T}_{ij})_{;j} = 0$  is obtained as

$$\dot{\rho}_m + \dot{\rho}_{khde} + \left( \frac{\dot{A}}{A} + \frac{\dot{B}}{B} + \frac{\dot{C}}{C} \right) (\rho_m + (1 + \omega_{khde}) \rho_{khde}) + \left( \alpha \frac{\dot{B}}{B} + \beta \frac{\dot{C}}{C} \right) \rho_{khde} = 0. \quad (19)$$

On integration, Eq. (18) yields  $B = k_1 C$ , where  $k_1$  is an integration constant. It can be taken as unity, without loss of any generality, so that we have

$$B = C. \quad (20)$$

Given the Eq. (20), the field equations (14) to (17) reduce to

$$2 \frac{\ddot{B}}{B} + \frac{\dot{B}^2}{B^2} + \frac{1}{A^2} = -\omega_{khde} \rho_{khde} \quad (21)$$

$$\frac{\ddot{A}}{A} + \frac{\ddot{B}}{B} + \frac{\dot{A}\dot{B}}{AB} - \frac{1}{A^2} = -(\omega_{khde} + \alpha) \rho_{khde} \tag{22}$$

$$\frac{\ddot{A}}{A} + \frac{\ddot{B}}{B} + \frac{\dot{A}\dot{B}}{AB} - \frac{1}{A^2} = -(\omega_{khde} + \beta) \rho_{khde} \tag{23}$$

$$2\frac{\dot{A}\dot{B}}{AB} + \frac{\dot{B}^2}{B^2} - \frac{1}{A^2} = (\rho_{khde} + \rho_m). \tag{24}$$

From Eqs. (22) and (23), we obtain

$$\alpha = \beta. \tag{25}$$

The reason for this is that the model exhibits isotropy in the y and z directions, resulting in the elimination of any deviations from the equation of state of dark energy. Based on Equation (25), the field equations (21)-(24) form a set of three distinct equations involving six variables:  $A, B, \rho_{khde}, \omega_{khde}, \rho_m$ , and  $\alpha$ . To get a predictable outcome for the complex and nonlinear field equations in our model, we impose the following reasonable physical constraints:

Here, we consider the fact that expansion scalar  $\theta$  is directly proportional to shear scalar  $\sigma$  which leads to a relation between the metric potentials as follows:

$$B = A^k \tag{26}$$

$k$  represents a positive constant that accounts for the anisotropy of space-time. Collins et al. [61] have determined that in a spatially homogeneous space-time, the normal congruence to the homogeneous expansion adheres to the constraint that the ratio of the shear stress ( $\sigma$ ) to the Hubble parameter ( $H$ ) remains constant.

Using the relation (26) in Eqs. (21) and (22), we obtain

$$\dot{A}A^{2k} = A_0 \exp \int \left\{ \frac{A}{(k-1)\dot{A}} \left( \frac{-2}{A^2} + \alpha \rho_{khde} \right) \right\} dt. \tag{27}$$

Recently, it has been common to assume that the skewness parameter is a function of the energy density of dark energy, in order to obtain a more comprehensive and specific solution. This assumption has been made by Akarsu and Kilinc [62], as well as Sharif and Zubair [63]. To get the explicit solution for Eq. (27), we use the assumption that there is a relationship between the skewness parameter  $\alpha(t)$  and the energy density of dark energy (DE), denoted as  $\rho_{khde}$

$$\alpha(t) = \frac{1}{\rho_{khde}} \left( \frac{2}{A^2} + \alpha_0(k-1) \frac{\dot{A}}{A} \right) \tag{28}$$

where  $\alpha_0$  is an arbitrary constant. These kinds of assumptions have been taken by several authors in literature [64]-[66]. Hence, from Eqs. (27) and (28) we find the metric potentials as

$$A = \left( \frac{A_0(2k+1)}{\alpha_0} \exp(\alpha_0 t) + (2k+1)A_1 \right)^{\frac{1}{2k+1}}$$

$$B = C = \left( \frac{A_0(2k+1)}{\alpha_0} \exp(\alpha_0 t) + (2k+1)A_1 \right)^{\frac{k}{2k+1}}. \tag{29}$$

Here  $A_0$  and  $A_1$  integrating constants. Now metric (4), with the help of metric potentials in Eq. (29), can be written as

$$ds^2 = dt^2 - \left( \frac{A_0(2k+1)}{\alpha_0} \exp(\alpha_0 t) + (2k+1)A_1 \right)^{\frac{2}{2k+1}} dx^2$$

$$- \left( \frac{A_0(2k+1)}{\alpha_0} \exp(\alpha_0 t) + (2k+1)A_1 \right)^{\frac{2k}{2k+1}} (e^{2x} dy^2 + e^{-2x} dz^2). \tag{30}$$

Eq. (29) represents a spatially homogeneous and anisotropic BT- $VI_0$  KHDE model within the framework of GR with the following properties along with the physical parameters given in the next sections. The average scale factor and volume of the model are, respectively, given by

$$a(t) = \left( \frac{A_0(2k+1)}{\alpha_0} \exp(\alpha_0 t) + (2k+1)A_1 \right)^{\frac{1}{3}} \tag{31}$$

$$V = \left( \frac{A_0(2k+1)}{\alpha_0} \exp(\alpha_0 t) + (2k+1)A_1 \right) \quad (32)$$

The average Hubble's parameter  $H$  and expansion scalar  $\theta$  are obtained as

$$H = 3\theta = \frac{(2k+1)A_0 \exp(\alpha_0 t)}{3 \left( \frac{A_0(2k+1)}{\alpha_0} \exp(\alpha_0 t) + (2k+1)A_1 \right)} \quad (33)$$

The shear scalar  $\sigma^2$  and average anisotropic parameter  $A_h$  are given by

$$\sigma^2 = \frac{A_1^2(k-1)^2 e^{2(\alpha_0 t)}}{3 \left( \frac{A_0(2k+1)}{\alpha_0} \exp(\alpha_0 t) + (2k+1)A_1 \right)^2} \quad (34)$$

$$A_h = \frac{2(k-1)^2}{(2k+1)^2}. \quad (35)$$

The statistics above demonstrate that as time ( $t$ ) advances, both the spatial volume and average scale factor of the universe exhibit exponential growth, indicating the expansion of the universe. Furthermore, during the first epoch, which is when  $t=0$ , all values become finite. However, as  $t$  approaches infinity, they diverge. It is worth mentioning that when  $k=1$ , the model becomes shear-free and isotropic, as shown by the conditions  $\sigma^2=0$  and  $A_h=0$ .

According to the HDE theory, for DE to be responsible for the current rapid expansion of the Universe, the total amount of vacuum energy contained inside a box of size  $L \propto \lambda_3$  should not exceed the energy of a black hole of the same size, as determined by the Kaniadakis black hole entropy equation (Eq. (2)). Subsequently, an individual acquires

$$\Lambda^4 \equiv \rho_{khde} \propto \frac{S_{\mathcal{K}}}{\mathcal{L}^4} \quad (36)$$

for the vacuum energy  $\rho_{khde}$ . Now, taking the Hubble horizon of the universe as the IR cutoff (i.e.,  $L = \frac{1}{H} A = \frac{4\pi}{H^2}$ ),

$$\rho_{khde} = \frac{3C^2 H^4}{\mathcal{K}} \sinh \left( \frac{\pi \mathcal{K}}{H^2} \right) \quad (37)$$

where the constant  $C^2$  is unknown,  $\mathcal{K}$  belongs to a set of real numbers, and  $H = \frac{\dot{a}}{a}$  is the Hubble parameter. Now, it is clear that we have  $\rho_{khde} \rightarrow \frac{3C^2 H^4}{\mathcal{K}}$  (the well-known Bekenstein entropy-based HDE) when  $k \rightarrow 0$ . Considering the pressureless fluid (with energy density  $\rho_m$ ) and the dark energy candidate (with pressure  $p_{khde}$  and density  $\rho_{khde}$ ).

The fractional energy densities of matter ( $\Omega_m$ ) and DE ( $\Omega_{khde}$ ) are given as

$$\Omega_m = \frac{\rho_m}{\rho_{cr}} = \frac{\rho_m}{3H^2} \quad \text{and} \quad \Omega_{khde} = \frac{\rho_{khde}}{\rho_{cr}} = \frac{C^2 H^2}{\mathcal{K}} \sinh \left( \frac{\pi \mathcal{K}}{H^2} \right), \quad (38)$$

$\rho_{cr}$  is the critical energy density.

We are considering non-interacting DE and matter in this case. As a result, we have from Eq. (19) that both of these are conserved individually

$$\dot{\rho}_m + 3H\rho_m = 0, \quad (39)$$

$$\dot{\rho}_{khde} + 3H(1 + \omega_{khde})\rho_{khde} + \frac{6kH}{2k+1} \left( \frac{2}{A^2} + \frac{\alpha_0(k-1)\dot{3}H}{2k+1} \right) = 0. \quad (40)$$

Differentiating Eq. (37) concerning time, we obtain

$$\dot{\rho}_{khde} = \frac{\rho_{khde} \dot{H}}{H^2} \left( 4H - \frac{2\pi \mathcal{K}}{H} \coth \left( \frac{\pi \mathcal{K}}{H^2} \right) \right). \quad (41)$$

Given Eqs. (33) and (41), from Eq. (40), we obtain the EoS parameter of KHDE as

$$\omega_{khde} = -1 - \frac{2\dot{H}}{3H^2} \left( 2 - \frac{\pi \mathcal{K}}{H^2} \coth \left( \frac{\pi \mathcal{K}}{H^2} \right) \right) - \frac{2k}{3(2k+1)H^2 \Omega_{khde}} \left[ \frac{2}{A^2} + \frac{3H\alpha_0(k-1)}{2k+1} \right] \quad (42)$$

where

$$\dot{H} = \frac{(2k+1)^2 A_0^2 \exp(2\alpha_0 t)}{3 \left( \frac{A_0(2k+1)}{\alpha_0} \exp(\alpha_0 t) + (2k+1)A_1 \right)^2} + \frac{(2k+1)A_0 \alpha_0 \exp(\alpha_0 t)}{3 \left( \frac{A_0(2k+1)}{\alpha_0} \exp(\alpha_0 t) + (2k+1)A_1 \right)}. \quad (43)$$

Here metric potential  $A(t)$ , Hubble parameter  $H(t)$  and fractional energy density of KHDE  $\Omega_{khde}$  are respectively given in Eqs. (29), (33) and (38).

### 3. COSMOLOGICAL PARAMETERS

In this section, we explore the expanding behaviour of the universe through well-known cosmological parameters like equation of state (EoS)  $\omega_{khde}$ , squared sound speed  $v_s^2$ , deceleration  $q$  parameters and cosmological planes such as  $\omega_{khde} - \omega'_{khde}$ , statefinders ( $r - s$ ) and  $r - q$  for the constructed anisotropic KHDE model.

#### EoS parameter

The equation of state parameter ( $\omega$ ) is often used to classify the different stages of the expanding universe. Specifically, the shift from decelerated to accelerated phases encompasses DE and radiation-dominated epochs. The equation of state (EoS) parameter, denoted by  $\omega = \frac{p}{\rho}$ , is defined as the ratio of pressure ( $p$ ) to energy density ( $\rho$ ) of the matter distribution. The decelerated and accelerated phases include the following periods:

- *Decelerated phase:* Cold dark matter or dust fluid  $\omega = 0$ , radiation era  $0 < \omega < \frac{1}{3}$  and stiff fluid  $\omega = 1$ .
- *Accelerated phase:* Cosmological constant/vacuum era  $\omega = -1$ , quintessence  $-1 < \omega < -\frac{1}{3}$ , phantom era  $\omega < -1$  and quintom era (combination of both quintessence and phantom).

The EoS parameter of KHDE with Hubble horizon cutoff is given in Eq. (42). In Fig. 1, we investigate the evolution of EoS parameter  $\omega_{khde}$  in terms of redshift  $z$  for different values of  $\mathcal{C}$ . Fig. 1 shows that initially  $\omega_{khde}$  starts from matter dominated era, varies in quintessence region  $-1 < \omega_{khde} < -1/3$  and finally it becomes  $-1$ , which means the model becomes  $\Lambda$ CDM model at late times.

#### Squared sound speed

The squared speed of the sound parameter is defined as

$$v_s^2 = \frac{\dot{p}_{khde}}{\dot{\rho}_{khde}} = \omega_{khde} + \frac{\rho_{khde}}{\dot{\rho}_{khde}} \dot{\omega}_{khde}. \tag{44}$$

This parameter is useful in discussing the stability of DE models depending upon its sign. The positive signature of  $v_s^2$  determines a stable DE model otherwise the model becomes unstable.

Using energy density and EoS parameter given in the Eqs. (37) and (42) in the squared sound speed expression ( $v_s^2$ ) Eq. (44), we analyze  $v_s^2$  graphically for our model. Fig. 2 elaborates the plot of  $v_s^2$  versus redshift  $z$ . Initially, the trajectories represent positive behaviour and negative at the present epoch and late times. Hence, this shows that our model is stable at the initial epoch and unstable at present and late times.

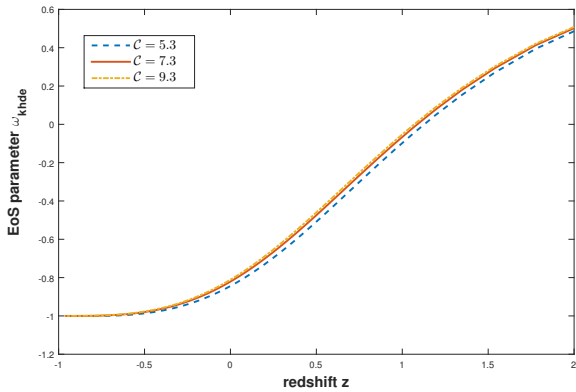


**Figure 1.** Plot of EoS parameter  $\omega_{de}$  versus redshift  $z$  for  $k = 0.98$ ,  $A_1 = -0.04$ ,  $\alpha_0 = 0.85$ ,  $A_0 = 0.04$  and  $\mathcal{K} = 0.01$ .

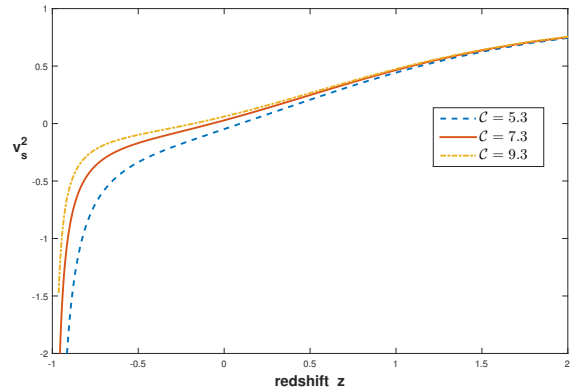


**Figure 2.** Plot of  $v_s^2$  versus redshift  $z$  for  $k = 0.98$ ,  $A_1 = -0.04$ ,  $\alpha_0 = 0.85$ ,  $A_0 = 0.04$  and  $\mathcal{K} = 0.01$ .

#### $\omega_{khde} - \omega'_{khde}$ plane

We analyze the  $\omega_{khde} - \omega'_{khde}$  plane, where  $\omega'_{khde}$  represents the evolutionary mode of the equation of state parameter  $\omega_{khde}$ , and the prime symbol indicates differentiation concerning the natural logarithm of the scale factor ' $\ln a$ '. Caldwell and Linder [67] have suggested using this framework to investigate the cosmic progression of the quintessence dark energy scenario. Furthermore, it has been noted that the  $\omega_{khde} - \omega'_{khde}$  plane may be divided into two distinct regions: thawing ( $\omega_{khde} < 0$ ,  $\omega'_{khde} > 0$ ) and freezing ( $\omega_{khde} < 0$ ,  $\omega'_{khde} < 0$ ). The freezing zone demonstrates a more rapid period of cosmic expansion compared to the thawing region.

Figure 3 examines the relationship between the  $\omega_{khde} - \omega'_{khde}$  plane and the KHDE model, specifically for various values of  $\mathcal{C}$ . Figure 3 illustrates that the  $\omega_{khde} - \omega'_{khde}$  plane corresponds to the area where freezing occurs for all three parameter values. Contemporary cosmological measurements indicate that the freezing zone reveals a period of greater cosmic acceleration compared to the thawing region. Therefore, the  $\omega_{khde} - \omega'_{khde}$  plane of our model demonstrates cosmic acceleration in the freezing area and aligns well with the facts.

### Energy conditions

The investigation of energy conditions was began by the Raychaudhuri equations, which are essential in any examination of the alignment of null and time-like geodesics. The energy requirements are used to demonstrate other general theorems about the behavior of powerful gravitational fields. The energy situations often seen are as follows:

Dominant energy condition (DEC):  $\rho_{de} \geq 0, \rho_{de} \pm p_{de} \geq 0$ .

Strong energy conditions (SEC) :  $\rho_{de} + p_{de} \geq 0, \rho_{de} + 3p_{de} \geq 0$ ,

Null energy conditions (NEC):  $\rho_{de} + p_{de} \geq 0$ ,

Weak energy conditions (WEC):  $\rho_{de} \geq 0, \rho_{de} + p_{de} \geq 0$ ,

Figure 4 illustrates the energy conditions of our KHDE model. There is an obvious violation of the NEC, leading to the model resulting in a Big Rip. Furthermore, it is seen that the WEC satisfies the condition  $\rho_{de} \geq 0$ . Furthermore, Figure 4 demonstrates that the DEC  $\rho_{de} + p_{de}$  is not fulfilled. Furthermore, our model violates the SEC regulations, which are deemed suitable. This phenomenon, resulting from the universe's acceleration in its latter stages, aligns with current observational findings.

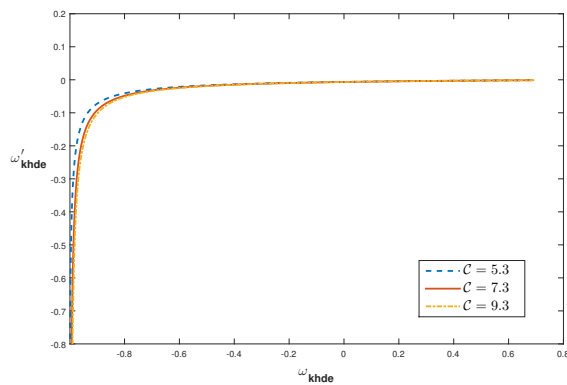


**Figure 3.** Plot of  $\omega_{de} - \omega'_{de}$  plane for  $k = 0.98$ ,  $A_1 = -0.04$ ,  $\alpha_0 = 0.85$ ,  $A_0 = 0.04$  and  $\mathcal{K} = 0.01$ .

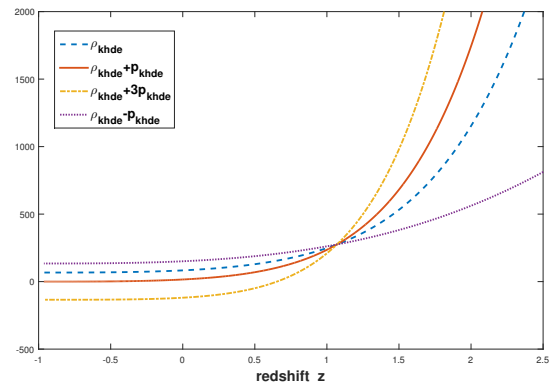


**Figure 4.** Plot of energy conditions versus redshift  $z$  for  $k = 0.98$ ,  $A_1 = -0.04$ ,  $\alpha_0 = 0.85$ ,  $A_0 = 0.04$ ,  $\mathcal{C} = 9.3$  and  $\mathcal{K} = 0.01$ .

### Deceleration parameter

The nature of the expansion of the universe can be estimated using the dimensionless cosmological parameter known as the deceleration parameter (DP). It defined as

$$q = -1 - \frac{\dot{H}}{H^2}. \quad (45)$$

For positive values of DP, the model decelerates in the standard way whereas for  $q = 0$  the model expands at a constant rate. The model shows accelerated expansion for  $-1 \leq q < 0$  and a super exponential expansion for  $q < -1$ . The deceleration parameter can be obtained as

$$q = -1 - \frac{3(2k+1)A_1\alpha_0}{(2k+1)\alpha_0 \exp(\alpha_0 t)}. \quad (46)$$

Figure 5 displays the relationship between the deceleration parameter  $q$  and the redshift  $z$  for different values of  $A_1$ . It is important to highlight that the model demonstrates a seamless transition from the universe's initial decelerated phase to its present accelerated phase. Within the specified range of  $0.5 < z < 0.85$ , the universe transitioned from a state of deceleration to a state of acceleration. This aligns with previous findings in the field of cosmology [68, 69]. The transition redshift ( $z_t$ ) from decelerating to accelerating expansion has been reported to be between 0.3 and 0.8, with a 95% confidence level. Additionally, it has been determined that the redshift for accelerating expansion ( $z_{acc}$ ) is greater than 0.14 in the most conservative scenario.

### Statefinder parameters

The dynamic expansion of the universe may be accurately characterized by the Hubble and deceleration parameters. Nevertheless, several dynamical dark energy models have identical parameter values at the current period. As a result, these factors were unsuccessful in determining the most suitable model among the several dynamical dark energy theories. Sahni et al. [70] developed a set of dimensionless cosmological parameters called statefinders, which are defined as follows:

$$r = \frac{\ddot{a}}{aH^3}, \quad s = \frac{r-1}{3(q-\frac{1}{2})}. \tag{47}$$

These statefinders establish a correspondence with the  $\Lambda$ CDM and CDM models for  $(r, s) = (1, 0)$  and  $(r, s) = (1, 1)$ , respectively. If the trajectories of  $r - s$  belong to the region  $s > 0$  and  $r < 1$ , then the model belongs to the phantom and quintessence phases whereas the Chaplygin gas model appears for  $r > 1$  with  $s < 0$ . The statefinders are obtained as

$$r = 10 + \frac{(A_0 \exp(\alpha_0 t) + A_1 \alpha_0)^2}{\alpha_0^2 \exp(2\alpha_0 t)}; \quad s = \frac{9 + \frac{(A_0 \exp(\alpha_0 t) + A_1 \alpha_0)^2}{\alpha_0^2 \exp(2\alpha_0 t)}}{3 \left( -\frac{3}{2} - \frac{3(2k+1)A_1 \alpha_0}{(2k+1)\alpha_0 \exp(\alpha_0 t)} \right)}. \tag{48}$$

Fig. 6 incorporates the trajectories of  $(r, s)$  parameters. It can be observed that the parameter ‘s’ is both positive and negative for all values of  $r$ . This implies that the KHDE model achieved a correspondence with the Chaplygin gas model, quintessence and phantom models. Also, the  $r - s$  plane corresponds to  $\Lambda$ CDM limit at late times.

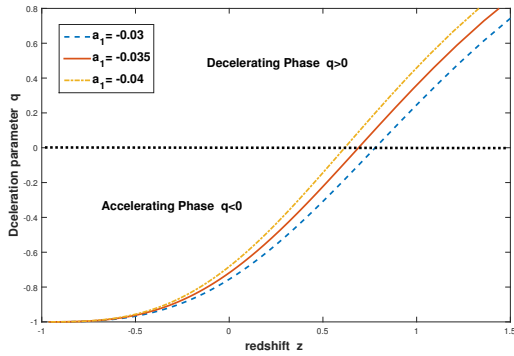


**Figure 5.** Plot of deceleration parameter  $q$  versus redshift  $z$  for  $k = 0.98$ ,  $A_1 = -0.04$  and  $\alpha_0 = 0.85$ .

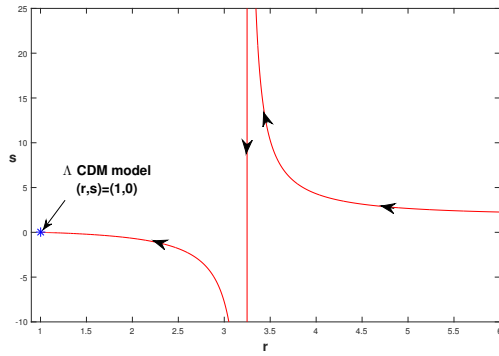


**Figure 6.** Plot of  $r - s$  plane for  $k = 0.98$ ,  $A_1 = -0.04$  and  $\alpha_0 = 0.85$ .

### $r - q$ plane

Figure 7 depicts the development of our model in the  $r - q$  plane. The values  $(r, q) = (1, 0.5)$  represent standard cold dark matter (SCDM) whereas  $(r, q) = (1, -1)$  represents the steady state (SS) model. The  $\Lambda$ CDM model evolves along the dotted line (see Fig. 7) from a fixed point in the SCDM model to a fixed point in the SS model. At late times, our model comes close to the SS model. The  $r - q$  trajectory of our model is found to be quite comparable to the DE models previously presented in the literature [71, 72]. In Fig. 7, we plot the trajectories in the  $r - q$  plane. It can be observed from the figure that our KHDE model always approaches the study state model, i.e.,  $(r, q) = (1, -1)$  as  $\Lambda$ CDM model approach in the later epochs.

## 4. DISCUSSION AND CONCLUSION

This study investigates the Kaniadakis holographic dark energy within the context of anisotropic Bianchi type- $V_{I_0}$  space-time in general relativity. In this case, we have regarded the Hubble horizon as the infrared cutoff. We have examined well-recognized cosmological parameters, including the equation of state (EoS), deceleration parameter, and squared speed of sound parameter. Additionally, we have explored cosmological planes such as the  $\omega_{khde} - \omega'_{khde}$  plane, the statefinder  $(r - s)$  plane, and the  $r - q$  plane. Our findings have been condensed into the following summary:

- The EoS parameter  $\omega_{khde}$  of the KHDE model initially starts from the matter-dominated era, varies in quintessence region  $-1 < \omega_{khde} < -1/3$  and finally it becomes  $-1$ , which means the model becomes  $\Lambda$ CDM



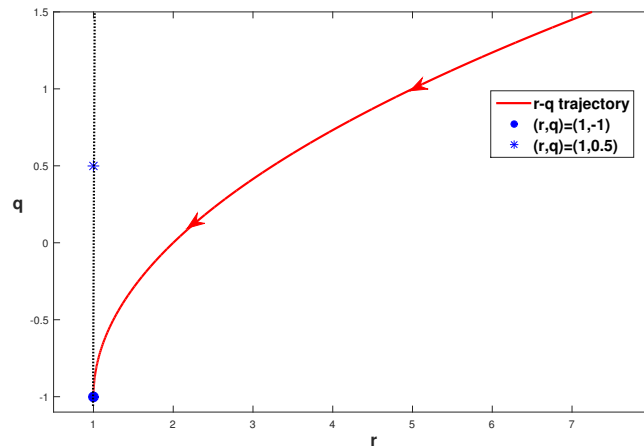


**Figure 7.** Plot of the  $r - q$  plane for  $k = 0.98$ ,  $A_1 = -0.04$  and  $\alpha_0 = 0.85$ .

model at late times. We have made a comparison of our results with present Planck collaboration data (2018) [73] where the limits on the EoS parameter are given as

$$\begin{aligned}\omega_{khde} &= -1.56^{+0.60}_{-0.48} \text{ (Planck + TT + lowE)} \\ \omega_{khde} &= -1.58^{+0.52}_{-0.41} \text{ (Planck + TT, TE, EE + lowE)} \\ \omega_{khde} &= -1.57^{+0.50}_{-0.40} \text{ (Planck + TT, TE, EE + lowE + lensing)} \\ \omega_{khde} &= -1.04^{+0.10}_{-0.10} \text{ (Planck + TT, TE, EE + lowE + lensing + BAO)}.\end{aligned}$$

It can be seen that the results for the EoS parameter of our model are consistent with the Planck Collaboration data.

- The  $\omega_{khde} - \omega'_{khde}$  plane (Fig. 3) depicts the area where freezing occurs for all three parameter values. Contemporary cosmological measurements indicate that the freezing zone reveals a period of greater cosmic acceleration compared to the thawing region. Therefore, the  $\omega_{khde} - \omega'_{khde}$  plane of our model demonstrates cosmic acceleration in the freezing area and aligns well with the facts. The paths of the  $\omega_{khde} - \omega'_{khde}$  plane, as predicted by our model, align with the observed data [74, 75]





$$\omega_{khde} = -1.13^{+0.24}_{-0.25}, \omega'_{khde} < 1.32 \text{ (Planck + WP + BAO)}.$$

- The squared sound speed trajectories exhibit positive behaviour initially and negative behaviour at the current epoch and late periods. Therefore, this demonstrates that our model is steady throughout the beginning period but becomes unsteady during the present and late times. The violation of the NEC leads to the occurrence of a Big Rip in the model. Furthermore, it is seen that the WEC satisfies the condition  $\rho_{de} \geq 0$ . Furthermore, the condition of the DEC  $\rho_{de} + p_{de}$  is not met. Furthermore, our model violates the SEC regulations, which are deemed suitable. This phenomenon, resulting from the universe's acceleration in its latter stages, aligns with current observational findings.
- Our model demonstrates a smooth transition from the universe's initial decelerated phase to its present accelerated phase. Within the specified range of  $0.5 < z < 0.85$ , the universe transitioned from a state of deceleration to a state of acceleration. This aligns with previous findings in the field of cosmology [68, 69]. The present value of the deceleration parameter is  $\approx -0.82$  which is by the observational data (Capozziello et al. [76]) given as  $q = -0.930 \pm 0.218$  ( $BAO + Masers + TDSL + Pantheon + H_z$ ),  $q = -1.2037 \pm 0.175$  ( $BAO + Masers + TDSL + Pantheon + H_0 + H_z$ ). It can be observed from the  $r - s$  plane that our model achieved a correspondence with the Chaplygin gas model, quintessence and phantom models. Also, the  $r - s$  plane corresponds to  $\Lambda$ CDM limit at late times. It can be seen from the  $r - q$  plane that our KHDE model always approaches the study state model, i.e.,  $(r, q) = (1, -1)$  as  $\Lambda$ CDM model approach in the later epochs.

### Acknowledgments

Y. Aditya is thankful to the National Board for Higher Mathematics, Department of Atomic Energy, Govt. of India for its financial support under the grant No: 02011/8/2023 NBHM(R.P.)/R & D II/3073.

## ORCID

 B. Ganeswara Rao, <https://orcid.org/0009-0007-4539-9130>;  Dipana Jyoti Mohanty, <https://orcid.org/0000-0002-1783-4090>;  Y. Aditya, <https://orcid.org/0000-0002-5468-9697>;  U.Y. Divya Prasanthi, <https://orcid.org/0009-0004-5397-050X>

## REFERENCES

- [1] S. Perlmutter, et al., *Astrophys. J.* **517**, 565 (1999). <https://doi.org/10.1086/307221>
- [2] A.G. Riess, et al., *Astron. J.* **116**, 1009 (1998). <https://doi.org/10.1086/300499>
- [3] T. Koivisto, and D.F. Mota, *Phys. Rev. D*, **73**, 083502 (2006). <https://doi.org/10.1103/PhysRevD.73.083502>
- [4] E.J. Copeland, et al., *Int. J. Mod. Phys. D*, **15**, 1753 (2006). <https://doi.org/10.1142/S021827180600942X>
- [5] R.R. Caldwell, and M. Kamionkowski, *Ann. Rev. Nucl. Part. Sci.* **59**, 397 (2009). <https://doi.org/10.1146/annurev-nucl-010709-151330>
- [6] K. Bamba, et al., *Astrophys. Space Sci.* **342**, 155 (2012). <https://doi.org/10.1007/s10509-012-1181-8>
- [7] S. Nojiri, et al., *Phys. Rept.* **692**, 1 (2017). <https://doi.org/10.1016/j.physrep.2017.06.001>
- [8] B. Ratra, and P.J.E. Peebles, *Phys. Rev. D*, **37**, 3406 (1988). <https://doi.org/10.1103/PhysRevD.37.3406>
- [9] R.R. Caldwell, R. Dave, and P.J. Steinhardt, *Phys. Rev. Lett.* **80**, 1582 (1998). <https://doi.org/10.1103/PhysRevLett.80.1582>
- [10] T. Padmanabhan, *Phys. Rev. D*, **66**, 021301 (2002). <https://doi.org/10.1103/PhysRevD.66.021301>
- [11] C. Armendariz-Picon, V.F. Mukhanov, and P.J. Steinhardt, *Phys. Rev. Lett.* **85**, 4438 (2000). <https://doi.org/10.1103/PhysRevLett.85.4438>
- [12] J. Sadeghi, et al., *Int. J. Theor. Phys.* **55**, 81 (2016). <https://doi.org/10.1007/s10773-015-2635-x>
- [13] M. Li, *Phys. Lett. B*, **603**, 1 (2004). <https://doi.org/10.1016/j.physletb.2004.10.014>
- [14] L. Susskind, *J. Math. Phys.* **36**, 6377 (1995). <https://doi.org/10.1063/1.531249>
- [15] A. Cohen, and D. Kaplan, A. Nelson, *Phys. Rev. Lett.* **82**, 4971 (1999). <https://doi.org/10.1103/PhysRevLett.82.4971>
- [16] Z.K. Gao, et al., *Phys. Rev. D*, **74**, 127304 (2006). <https://doi.org/10.1103/PhysRevD.74.127304>
- [17] L.N. Granda, and A. Oliveros, *Phys. Lett. B*, **671**, 199 (2009). <https://doi.org/10.1016/j.physletb.2008.12.025>
- [18] H. Wei, and R.G. Cai, *Phys. Lett. B*, **660**, 113 (2008). <https://doi.org/10.1016/j.physletb.2007.12.030>
- [19] S. Nojiri, and S.D. Odintsov, *Gen. Rel. Grav.* **38**, 1285 (2006). <https://doi.org/10.1007/s10714-006-0301-6>
- [20] S. Nojiri, et al., *Phys. Lett. B*, **797**, 134829 (2019). <https://doi.org/10.1016/j.physletb.2019.134829>
- [21] M. Tavayef, A. Sheykhi, K. Bamba, and H. Moradpour, *Phys. Lett. B*, **781**, 195 (2018). <https://doi.org/10.1016/j.physletb.2018.04.001>
- [22] C. Tsallis, and L.J.L. Cirto, *Eur. Phys. J. C*, **73**, 2487 (2013). <https://doi.org/10.1140/epjc/s10052-013-2487-6>
- [23] A.S. Jahromi et al., *Phys. Lett. B*, **780**, 21 (2018). <https://doi.org/10.1016/j.physletb.2018.02.052>
- [24] H. Moradpour et al., *Eur. Phys. J. C*, **78**, 829 (2018). <https://doi.org/10.1140/epjc/s10052-018-6309-8>
- [25] D.R.K. Reddy, et al., *Astrophys Space Sci.* **361**, 356 (2016). <https://doi.org/10.1007/s10509-016-2938-2>
- [26] Y. Aditya, and D.R.K. Reddy, *Eur. Phys. J. C*, **78**, 619 (2018). <https://doi.org/10.1140/epjc/s10052-018-6074-8>
- [27] V.U.M. Rao, et al., *Results in Physics*, **10**, 469 (2018). <https://doi.org/10.1016/j.rinp.2018.06.027>
- [28] M.V. Santhi, et al., *Can. J. Phys*, **95**, 381 (2017). <https://doi.org/10.1139/cjp-2016-0781>
- [29] M.V. Santhi, et al., *Int. J. Theor. Phys.* **56**, 362 (2017). <https://doi.org/10.1007/s10773-016-3175-8>
- [30] K.D. Naidu, et al., *Eur. Phys. J. Plus*, **133**, 303 (2018). <https://doi.org/10.1140/epjp/i2018-12139-2>
- [31] Y. Aditya, et al., *Eur. Phys. J. C*, **79**, 1020 (2019). <https://doi.org/10.1140/epjc/s10052-019-7534-5>
- [32] S. Maity, U. Debnath, *Eur. Phys. J. Plus*, **134**, 514 (2019). <https://doi.org/10.1140/epjp/i2019-12884-6>
- [33] A. Iqbal, A. Jawad, *Physics of the Dark Universe*, **26**, 100349 (2019). <https://doi.org/10.1016/j.dark.2019.100349>
- [34] G. Kaniadakis, *Physica A: Stat. Mech. and its Appl.* **296**(3-4), 405 (2001). [https://doi.org/10.1016/S0378-4371\(01\)00184-4](https://doi.org/10.1016/S0378-4371(01)00184-4)
- [35] M. Masi, *Phys. Lett. A*, **338**, 217 (2005). <https://doi.org/10.1016/j.physleta.2005.01.094>
- [36] E.M. Abreu, et al., *EPL (Europhysics Letters)*, **124**, 30003 (2018). <https://doi.org/10.1209/0295-5075/124/30003>
- [37] H. Moradpour, et al. *Eur. Phys. J. C*, **80**, 1 (2020). <https://doi.org/10.1140/epjc/s10052-020-8307-x>

- [38] A. Jawad, and A.M. Sultan, Adv. High Energy Phys. **2021**, 5519028 (2021). <https://doi.org/10.1155/2021/5519028>
- [39] U.K. Sharma, et al., IJMPD, **31**, 2250013 (2022). <https://doi.org/10.1142/S0218271822500134>
- [40] N. Drepanou et al., ur. Phys. J. C, **82**, 449 (2022). <https://doi.org/10.1140/epjc/s10052-022-10415-9>
- [41] J. Sadeghi, et al., arXiv:2203.04375 (2022). <https://doi.org/10.48550/arXiv.2203.04375>
- [42] C.L. Bennett, et al., Astron. Astrophys. Suppl. Ser. **148**, 1 (2003). <https://doi.org/10.1086/377252>
- [43] O. Akarsu, and C.B. Kilinc, Astrophys. Space Sci. **326**, 315 (2010). <https://doi.org/10.1007/s10509-009-0254-9>
- [44] D.R.K. Reddy, et al., Can. J. Phys. **97**, 932 (2019). <https://doi.org/10.1139/cjp-2018-0403>
- [45] Y. Aditya, et al., Astrophys. Space Sci. **364**, 190 (2019). <https://doi.org/10.1007/s10509-019-3681-2>
- [46] Y. Aditya, and D.R.K. Reddy, Astrophys. Space Sci. **364**, 3 (2019). <https://doi.org/10.1007/s10509-018-3491-y>
- [47] K.D. Raju, et al., Astrophys. Space Sci. **365**, 45 (2020). <https://doi.org/10.1007/s10509-020-03753-1>
- [48] K.D. Raju, et al., Astrophys. Space Sci. **365**, 28 (2020). <https://doi.org/10.1007/s10509-020-3729-3>
- [49] Y. Aditya, et al., Ind. J. Phys. **95**, 383 (2021). <https://doi.org/10.1007/s12648-020-01722-6>
- [50] R.L. Naidu, et al., Astrophys. Space Sci. **365**, 91 (2020). <https://doi.org/10.1007/s10509-020-03796-4>
- [51] R.L. Naidu, et al., Ind. J. Phys. **85**, 101564 (2021). <https://doi.org/10.1016/j.newast.2020.101564>
- [52] K.D. Naidu, et al., Mod. Phys. A, **36**, 2150054 (2021). <https://dx.doi.org/10.1142/S0217732321500541>
- [53] Y. Aditya, et al., New Astr. **84**, 101504 (2021). <https://doi.org/10.1016/j.newast.2020.101504>
- [54] Y. Aditya, et al., Int. J. Mod. Phys. A, **37**, 2250107 (2022). <https://doi.org/10.1142/S0217751X2250107X>
- [55] M.P.V.V. Bhaskara Rao, et al., New Astr. **92**, 101733 (2022). <https://doi.org/10.1016/j.newast.2021.101733>
- [56] U.Y.D. Prasanthi, and Y. Aditya, Phys. Dark Univ. **31**, 100782 (2021). <https://doi.org/10.1016/j.dark.2021.100782>
- [57] U.Y.D. Prasanthi, and Y. Aditya, Results Phys. **17**, 103101 (2020). <https://doi.org/10.1016/j.rinp.2020.103101>
- [58] M.P.V.V. Bhaskara Rao, et al., Int. J. Mod. Phys. A, **36**, 2150260 (2021). <https://doi.org/10.1142/S0217751X21502602>
- [59] Y. Aditya, and U.Y.D. Prasanthi, Bulg. Astr. Journal, **38**, 52 (2023). <https://astro.bas.bg/AIJ/issues/n38/YAditya.pdf>
- [60] Y. Aditya, Bulg. Astr. Journal, **39**, 12 (2023). <https://astro.bas.bg/AIJ/issues/n39/YAditya.pdf>
- [61] C.B. Collins, et al., Gen. Relativ. Gravit. **12**, 805 (1980). <https://doi.org/10.1007/BF00763057>
- [62] O. Akarsu, and C.B. Kilinc, Gen. Relativ. Gravit. **42**, 119 (2010). <https://doi.org/10.1007/s10714-009-0821-y>
- [63] M. Sharif, and M. Zubair, Astrophys. Space Sci. **330**, 399 (2010). <https://doi.org/10.1007/s10509-010-0414-y>
- [64] M.V. Santhi, et al., Astrophys. Space Sci. **361**, 142 (2016). <https://doi.org/10.1007/s10509-016-2731-2>
- [65] M.V. Santhi, et al., Can. J. Phys. **95**, 179 (2017). <https://doi.org/10.1139/cjp-2016-0628>
- [66] Y. Aditya, and D.R.K. Reddy, Astrophys. Space Sci. **363**, 207 (2018). <https://doi.org/10.1007/s10509-018-3429-4>
- [67] R. Caldwell, and E.V. Linder, Phys. Rev. Lett. **95**, 141301 (2005). <https://doi.org/10.1103/PhysRevLett.95.141301>
- [68] S. Capozziello, et al., Phys. Rev. D, **90**, 044016 (2014). <https://doi.org/10.1103/PhysRevD.90.044016>
- [69] D. Muthukrishna, and D. Parkinson, JCAP, **11**, 052 (2016). <https://doi.org/10.1088/1475-7516/2016/11/052>
- [70] V. Sahni, et al., J. Exp. Theor. Phys. Lett. **77**, 201 (2003). <https://doi.org/10.1134/1.1574831>
- [71] Y. Aditya, et al., Int. J. Mod. Phys. A, **37**, 2250107 (2022). <https://doi.org/10.1142/S0217751X2250107X>
- [72] C.P. Singh, and P. Kumar, Astrophys. Space Sci. **361**, 157 (2016). <https://doi.org/10.1007/s10509-016-2740-1>
- [73] N. Aghanim, et al., [Plancks Collaboration] arXiv:1807.06209v2 (2018). <https://doi.org/10.48550/arXiv.1807.06209>
- [74] P.A.R. Ade, et al., Astrophys. **571**, A16 (2014). <https://doi.org/10.1051/0004-6361/201321591>
- [75] G.F. Hinshaw, et al., Astrophys. J. Suppl. **208**, 19 (2018). <https://doi.org/10.1088/0067-0049/208/2/19>
- [76] S. Capozziello, et al., MNRAS, **484**, 4484 (2019). <https://doi.org/10.1093/mnras/stz176>

КОСМОЛОГІЧНА ЕВОЛЮЦІЯ ГОЛОГРАФІЧНОЇ МОДЕЛІ ТЕМНОЇ ЕНЕРГІЇ  
КАНІАДАКІСА ТИПУ БІАНКІ- $V I_0$ Б. Ганешвара Рао<sup>a,b</sup>, Діпана Джіоті Моханті<sup>b</sup>, Ю. Адитья<sup>c</sup>, Ю.Й. Дів'я Прасанті<sup>d</sup><sup>a</sup> Департамент математики Шрі G.C.S.R. Коледж, Раджам-532127, Індія<sup>b</sup> Департамент математики, Університет GIET, Гунупур-765002, Індія<sup>c</sup> Департамент математики, Технологічний інститут GMR, Раджам-532127, Індія<sup>d</sup> Департамент статистики і математики, Коледж садівництва, д-р Y.S.R. Університет садівництва,  
Парватіпур-535502, Індія

Метою цієї статті є побудова анізотропної та просторово однорідної голографічної моделі темної енергії Каніадакіса типу Біанкі  $V I_0$  в загальній теорії відносності. Для цього ми розглядаємо обрії Хаббла як межу інфрачервоного випромінювання. Щоб отримати детермінований розв'язок рівнянь поля моделі, ми припускаємо зв'язок між метричними потенціалами, який призводить до експоненціального розв'язку та прискореного розширення. Щоб дослідити фізичну поведінку нашої моделі темної енергії, ми отримуємо деякі важливі космологічні параметри, такі як Хаббл, уповільнення, рівняння стану та вимірювач стану, а також  $\omega_{khde} - \omega'_{khde}$ ,  $r - s$  і  $r - q$  площини. Ми також включили аналіз стабільності для моделі темної енергії через квадрат швидкості звуку. Помічено, що рівняння параметра стану показує модель  $\Lambda$ CDM у пізній час. Крім того, квадрат швидкості звуку дає стабільність моделі КНДЕ на початковій епосі, а модель є нестабільною на пізніх етапах. Діагностичні параметри вимірювача стану та параметри уповільнення демонструють плавний перехід Всесвіту від фази уповільнення до поточного прискореного розширення Всесвіту, а також відповідають моделі  $\Lambda$ CDM у пізні часи. Усі ці космологічні параметри підтверджують останні дані спостережень.

**Ключові слова:** модель темної енергії типу Bianchi- $V I_0$ ; загальна теорія відносності; космологія; голографічна темна енергія Каніадакіса